ELSEVIER

Sensors and Actuators B 38–39 (1997) 277–282

SENSORS AND ACTUATORS B CHEMICAL

Integrated optical Mach–Zehnder interferometers as simazine immunoprobes

B. Drapp [a], J. Piehler [a], A. Brecht [a,*], G. Gauglitz [a], B.J. Luff [b], J.S. Wilkinson [b], J. Ingenhoff [c]

[a] *Institute for Physical and Theoretical Chemistry, University of Tübingen, Auf der Morgenstelle 8, D-72076 Tübingen, Germany*

[b] *Optoelectronics Research Centre, University of Southampton, Highfield, Southampton SO17 1BJ, UK*

[c] *IOT Entwicklungsgesellschaft für Integrierte Optik Technologie mbH, Bruchsaler-Straße 22, D-68753 Waghäusel-Kirrlach, Germany*

Abstract

Immunoassay has become a versatile tool in several fields of analytical chemistry. We describe the characterization and the application of different integrated optical channel waveguide Mach–Zehnder interferometers (MZIs) as label-free immunoprobes. The performance of the classical MZI is compared with that of a modified structure which incorporates a 3×3 coupler. Characterization of the devices demonstrates a dramatic improvement gained by using the 3×3 coupler. Two main advantages are achieved by the modified device. First, the possibility of referencing the output signal allows the elimination of signal fluctuations due to coupling and light-source instabilities. An increase of the signal-to-noise ratio by a factor of up to 10 is achieved. Secondly, the phase shift between the three outputs allows unambiguous detection with optimum sensitivity. For the detection of the herbicide simazine, the functional properties of the transducer surface are optimized by an appropriate chemical modification. Using this improved device, a simazine immunoassay has been carried out with a test midpoint of 0.3 ppb and a detection limit of approximately 0.1 ppb. The excellent performance, established manufacturing techniques and the potential for simplification and parallelization make the device attractive for further development.

Keywords: Integrated optical immunoprobes; Mach–Zehnder interferometers; 3×3 couplers

1. Introduction

Since the introduction of immunoassay in 1960, this technique has found increasing interest in the field of analytical chemistry. Immunoassay techniques achieve detection limits in the nanomolar range using simple, rapid and low-cost test formats [1]. In several fields, such as medical, food and environmental analysis, immunoassay techniques are already well established. In recent years efforts have been made towards further simplification of this method by applying label-free detection systems, in particular in the field of pesticide analysis in water [2–7]. The requirements for the application in this field are:

- a highly sensitive detection principle,
- a small and rugged set-up,
- the possibility for parallel detection of several analytes.

Detection systems based on evanescent-field interrogation have been applied with promising results to the field of immunoassay [8–10] and various integrated optical devices have been investigated [9,11–13]. Integrated optical devices have primarily been developed for use in telecommunication and signal processing. For this reason, a large variety of manufacturing processes is already established including ion-exchange and silica-on-silicon technology. Integrated optical sensor devices meet the requirements for sensor applications as they combine high sensitivity with potentially compact and simple instrumentation and a high degree of parallelization.

In this study we present the characterization and application of two different integrated optical sensor devices based on a Mach–Zehnder interferometer (MZI) structure with respect to pesticide immunoassay in water samples.

1.1. Detection principle

The principle of optical interrogation of affinity interaction at a surface is based on the difference in refractive index between water and organic matter. Increasing concentrations c of protein in an aqueous phase increase the refractive index of the mixture from 1.3 (pure water) with a typical increment of $dn/dc \approx 0.188$ ml g^{-1} [14]. The enrichment of protein at the surface of a waveguide due to a surface-bound affinity interaction leads to the formation of a protein film with a

* Corresponding author. Phone: +49 7071 294 667. Fax: +49 7071 296 910.

0925-4005/97/$17.00 © 1997 Published by Elsevier Science S.A. All rights reserved
PII S0925-4005(96)02123-5

refractive index of about 1.4 [15]. Protein binding at the surface of a waveguide therefore increases the average refractive index adjacent to the surface that is interrogated by the evanescent field. Hence, an evanescent-field microrefractometer can be used for the detection of affinity interactions. Label-free immunoassays can be carried out using such devices by detection of the inhibition of antibody binding to an immobilized analyte derivative. We have investigated two different types of integrated optical devices based on the MZI structure shown in Fig. 1.

A detailed description of the basic MZI principle is found in Ref. [16]. Application of various MZI devices for the detection of affinity interactions has been reported [5,11,17]. Typically, a monomode waveguide is split into two different arms, which are recombined after a distance of several millimetres. For sensing applications the surface of the device is covered with a patterned isolation layer in such a way that interaction with the evanescent field is possible only at one arm of the structure. Variation of the superstrate refractive index n_0 then changes the effective refractive index of this waveguide and therefore leads to a phase shift between the interferometer arms and to a change in the output intensity

$$\frac{I(\Delta\varphi)}{I_0}=\frac{1}{2}[1+\cos(lk_0\Delta n_{\text{eff}})] \quad (1)$$

(I_0 denotes the incoupled intensity, $I(\Delta\varphi)$ the measured intensity, l the length of the measuring window, Δn_{eff} the difference between the effective refractive indices in the measuring and the reference arm, and the wave vector $k_0=2\pi/\lambda$). As the output intensity of the interferometer follows a cosine function, the device sensitivity dI/dn_0 depends on the operating point of the intensity curve. If the operating point is near to an extremum of the cosine curve, the resultant reduction in sensitivity is a critical drawback for detecting very small phase shifts ($\ll\pi$) in applications involving small changes in the effective refractive index, e.g., detection of a few protein molecules binding at the device surface.

For this reason we have improved the classical design of the MZI by combining it with a 3×3 coupler structure as shown schematically in Fig. 2.

The main difference between the two devices is that, instead of recombining the two light beams of the interferometer in a simple Y-junction, mode coupling is used to exchange power from the two arms between the three outputs of the coupler. For sensing applications an ideal phase shift of $2\pi/3$ between all outputs can be achieved (Fig. 2). Using this technique, optimum sensitivity is obtained for the detection of small phase shifts ($\ll\pi$) by selecting the optimum output and an unambiguous detection of a change in effective refractive index is possible by comparing the phase shift of all three outputs.

A further advantage of incorporating the three-output directional coupler is gained by the fact that the total incoupled intensity is maintained for this type of interferometer. Hence, the sum of all three outputs remains constant and can be used for referencing the signal. This is particularly impor-

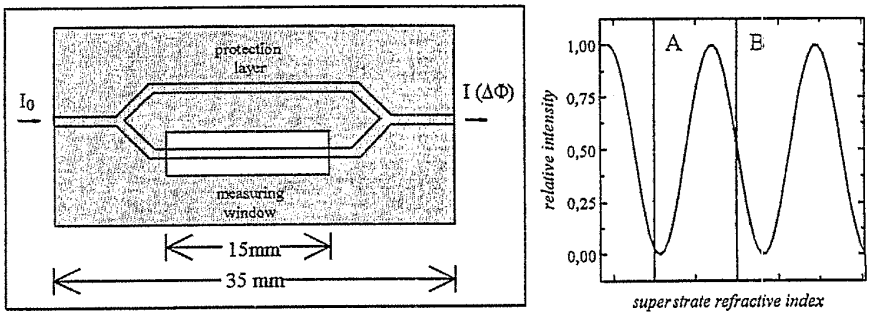

Fig. 1. Structure of the MZI and theoretical output intensity modulation with increasing refractive index n_0. At the operating point A the sensitivity dI/dn_0 is significantly lower than at the operating point B.

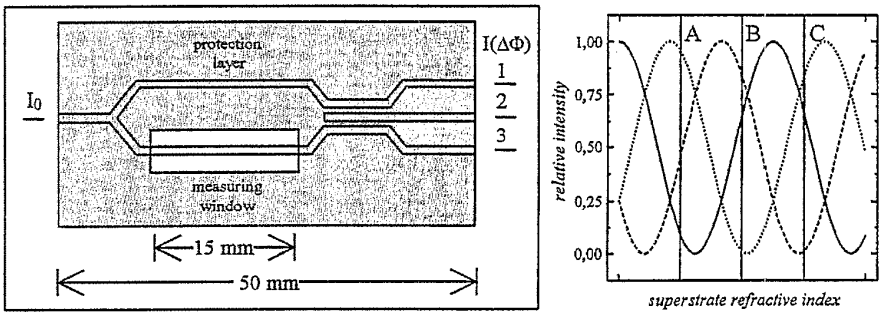

Fig. 2. Schematic of the modified MZI with integrated 3×3 coupler structure and the three phase-shifted output signals. At all operating points A, B and C one of the outputs provides satisfactory sensitivity.

tant if the stability of the light source or the incoupling is a critical parameter for the performance.

In this study, we compare the performance of the basic MZI device (referred to as MZI1 in the following) and the combined MZI/3 × 3-coupler structure (referred to as MZI2 in the following).

2. Experimental

2.1. Materials

Common chemicals for surface chemistry and biochemicals were purchased from Sigma, Deisenhofen, Germany and Fluka, Neu-Ulm, Germany. Silanes were obtained from ABCR, Karlsruhe, Germany. Amino dextran was prepared according to Ref. [20]. Simazine standard solutions (100 ng μl^{-1} in methanol) were purchased from Riedel de Haen.

Polyclonal sheep-anti-simazine antibodies and Fab fragments as well as the triazine derivative 4-chloro-6-(isopropylamino)-1,3,5-triazine-2-(6′-amino)caproic acid (CTCA) were kindly provided by Dr Ram Abuknesha, GEC Marconi Materials Technology, Hirst Division, Borehamwood, UK.

BGG36 glass substrates were supplied by Schott, Mainz, Germany. Teflon AF was purchased from DuPont De Nemours, Germany and Teflon FEP from Adtech, UK.

All protein samples were prepared in PBS (phosphate-buffered saline, pH 7.4). The standard samples for the immunoassay calibration were prepared in PBS from a single master solution of 100 $\mu g\ l^{-1}$.

2.2. Device fabrication

The integrated optical devices were designed and produced at the facilities of IOT by applying established processes. Monomode channel waveguides were produced in a BGG36 glass substrate with a refractive index of 1.6009 at 588 nm using a mask opening width of 1 μm by ion exchanging in a 10% Ag^+ ion salt melt at 316°C for 7 min. The devices were tempered at 250°C for 90 min (MZI1) and for 60 min (MZI2) directly after ion exchanging. A peak change in refractive index Δn of 0.075 was obtained by this treatment.

The surface of the MZI1 device was covered with a patterned SiO_2 protection layer using a plasma impulse CVD process [18]. For the MZI2 device the protection layer was achieved by patterning an evaporated Teflon layer (AF and FEP, refractive indices of 1.31) by a lift-off technique [19]. Using this patterning procedure, a window of 15 mm length was left open for the interaction with the analyte.

2.3. Experimental set-up

The principal experimental set-up for measurements with MZI1 is shown in Fig. 3. TM-polarized light from a semiconductor laser diode operating at 785 nm (HC 7812G, Hitachi, Germany) was end-fire coupled into the device using a microscope objective. The output light was coupled into a multimode fibre and detected with a photodiode (OSI 5K, Centronics). In the case of the MZI2 device, the outputs of the coupler were directly imaged onto three separate Si photodiodes (13DIS009, RS Components, UK). The output from each photodiode was measured using lock-in amplification (SR530, Stanford Research, USA). Data acquisition was carried out with a 80386 PC using a 12 bit A/D card (DAS1600, Keithly) for the MZI1 device and a GPIB interface for the MZI2 device. The samples (750 μl) were incubated in a flow-through system using flow-injection analysis (ASIA, ISMATEC, Zürich, Switzerland).

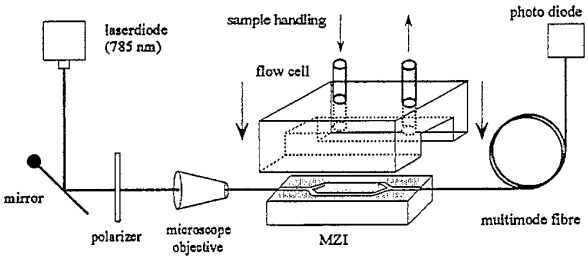

Fig. 3. Set-up for monitoring affinity interactions using MZI devices.

2.4. Assay formats

The variations of the output intensity of the devices due to changes in the cover refractive index were determined by incubation of aqueous solutions of calcium chloride or sucrose at various refractive indices between 1.333 and 1.4 (n_D).

The surface of the device was covalently modified with an analyte derivative for the detection of specific antibody binding. After silanization and activation, amino dextran was coupled covalently to shield the surface against non-specific adsorption. The analyte derivative (CTCA) was coupled to the remaining amino groups of the dextran. This modification procedure and the characterization of the functional properties has recently been described in detail [20]. The modified surface was characterized with respect to non-specific adsorption by incubation of 1 mg ml^{-1} ovalbumin. Specific binding was investigated by incubating an anti-triazine antibody at various concentrations. The specifically bound antibody was removed from the surface by incubation of 2 mg ml^{-1} pepsin at pH 1.9. A short pulse (10 s) of a mixture of acetonitrile, water and propionic acid (50:50:1) was frequently used in a second step to complete regeneration. Changes in the output intensity during binding of proteins and the regeneration procedures were monitored with a time resolution of 1–2 s.

Immunoassays were carried out using a binding-inhibition test format [21]. In a first step the antibody was incubated with the sample for at least 5 min to reach equilibrium occupation of the antibody binding sites. Then the transducer surface was exposed to the pre-incubated sample and binding of the remaining antibodies with free binding sites at the immobilized analyte derivative was monitored. The slope of

the binding curves was determined by linear regression and normalized with respect to the slope of the blank curve. Five different simazine concentrations logarithmically equidistant between 0.1 and 10 ppb were investigated. The response was determined three times for each concentration.

3. Results and discussion

3.1. Device performance

The response of the devices was characterized with respect to changes in superstrate refractive index by monitoring the variation in intensity during incubation solution at various refractive indices. A sensitivity to changes in the cover refractive index (in aqueous medium) $d\Phi/dn_0$ of 240π was found for MZI1 and 280π for MZI2, indicating slightly different properties of the MZI structures. A comparison of the three outputs of the MZI2 device is shown in Fig. 4.

Phase shifts of 2.6 rad between outputs 1 and 3 and a phase shift of 4.5 rad between outputs 1 and 2 were observed. The amplitudes of the intensity modulation are in a ratio of 2:1:2 between outputs 1, 2 and 3, indicating that the coupler structure is not ideally balanced. In Fig. 5 the advantage of using the 3×3 coupler for referencing the output signal is demonstrated by comparing the raw and the referenced signals.

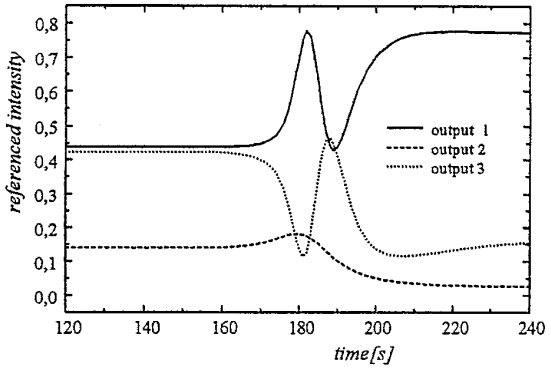

Fig. 4. Intensity modulation of the MZI2 device for a change from 1.3335 to 1.3464 in superstrate refractive index.

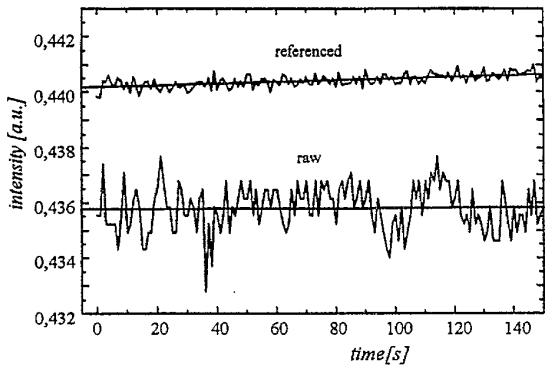

Fig. 5. Comparison of the raw and the referenced signal: a typical baseline interval for the MZI2 device.

Strong fluctuations are observed for the raw signal, which are significantly reduced in the referenced signal. The signal-to-noise ratio is thereby increased by a factor of 5–10 (depending on the stability of the raw signal) and long-term drift of the signal is drastically reduced. For the modified MZI2 device a detection limit for a change in superstrate refractive index of 1.5×10^{-6} was determined from the three-fold rms noise.

The masking of part of the MZI with a protective layer leads to a different effective refractive index of waveguide modes in the two arms and in consequence to an unbalanced interferometer structure. Unbalanced interferometer structures are more sensitive to temperature variations than fully balanced designs. However, in this study we did not observe significant perturbations. As the measurements are conducted using a flow-injection analyser in a well-controlled environment, temperature fluctuations over the duration of an assay are likely to be small.

3.2. Functional properties of the modified devices

Prior to application to immunoassays, the modified devices were characterized with respect to their interaction with non-specific and specific proteins. Very low non-specific protein adsorption occurred during incubation of ovalbumin at very high concentration (Fig. 6).

Specific binding is clearly detectable at low (30 nM) and high (300 nM) antibody concentrations (Fig. 7).

A constant binding rate is observed up to a phase shift of approximately π, indicating mass-transport-limited binding due to a high concentration of binding sites [22]. At the higher antibody concentration saturation of the binding curve is observed. The phase shift for maximum loading of approximately 6π for MZI1 and 3π for MZI2 indicates higher sensitivity of the MZI1 device to changes in surface coverage. However, the excellent signal-to-noise ratio and the lack of signal fluctuations again clearly demonstrate the greatly improved performance of the MZI2 device.

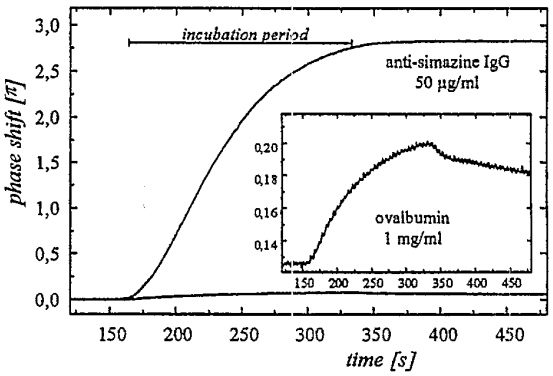

Fig. 6. Non-specific adsorption (shown enlarged in the inset) and specific binding at the modified device surface of MZI2.

For the immunoassay application the antibody concentration was optimized by investigating the signal obtained for decreasing concentrations. For the MZI1 device a working concentration of 2 μg ml^{-1} was chosen (Fig. 8) and a concentration of 0.35 μg ml^{-1} for MZI2. Due to the mass-transport-controlled binding rate at low antibody concentration, the signal does not depend on the absolute concentration of binding sites at the transducer surface but only on the concentration of free antibody binding sites. For this reason the surface modification allows more than 200 immunoassay cycles on the same device, as was shown for another silica-based transducer [4].

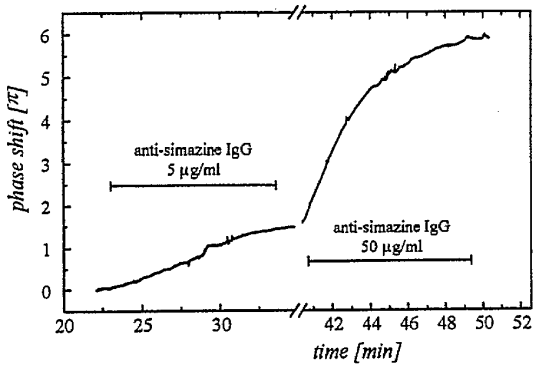

Fig. 7. Specific antibody in low-concentration (30 nM) and high-concentration (300 nM) binding at the modified surface (measured with MZI1).

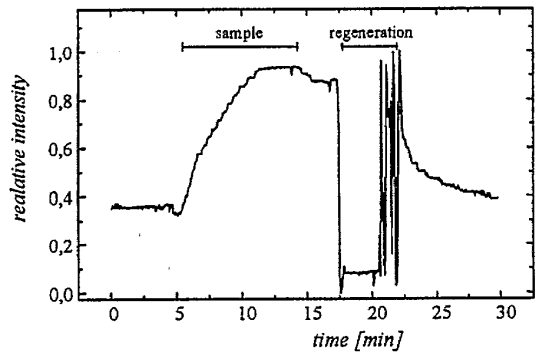

Fig. 8. Typical immunoassay test cycle including the injection of the antibody and the regeneration by pepsin, measured with the MZI1 device.

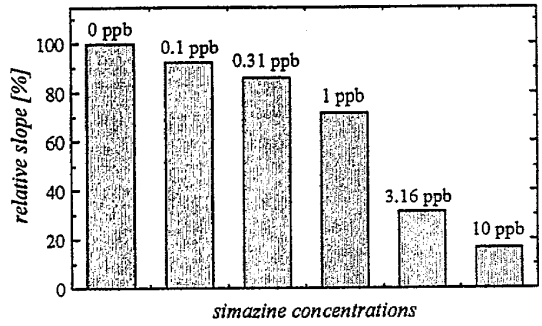

Fig. 9. Inhibition of antibody binding (2 μg ml^{-1} IgG) at various simazine concentrations measured with MZI1.

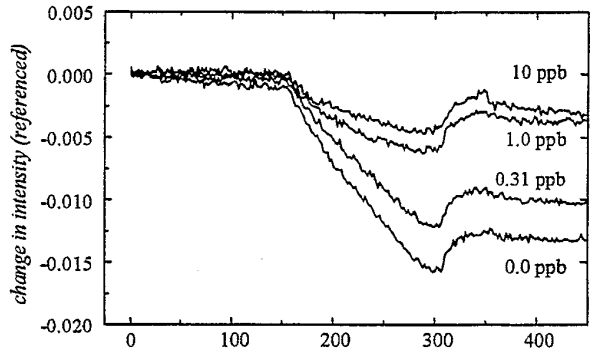

Fig. 10. Antibody binding (0.35 μg ml^{-1} anti-simazine Fab) at various simazine concentrations (measured with MZI2).

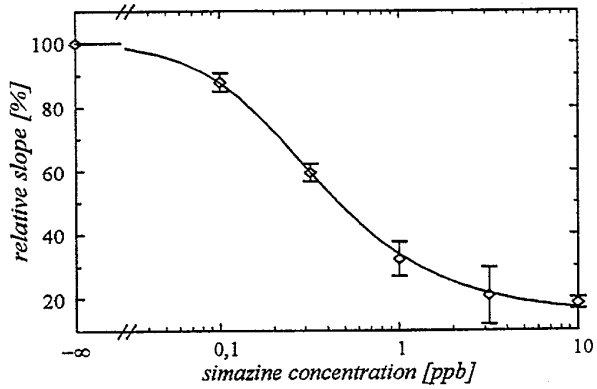

Fig. 11. Calibration curve for the simazine immunoassay obtained with the MZI2 device at 0.35 μg ml^{-1} anti-simazine Fab.

The reproducibility of the measurements with the MZI1 device was limited by strong coupling instabilities. However, antibody inhibition was unambiguously detected at an antibody concentration of 2 μg ml^{-1} (Fig. 9).

In the case of MZI2 excellent reproducibility of the measurements was observed even at the low antibody concentration of 0.35 μg ml^{-1}. Significant inhibition of antibody binding was detected even at analyte concentrations in the sub-ppb range (Fig. 10).

By plotting the relative slope of the linear binding curves versus the analyte concentration on a logarithmic scale, a typical immunoassay calibration curve was obtained (Fig. 11).

A test midpoint of 0.3 μg l^{-1} is found at this antibody concentration and the CV values were good overall. The limit of detection was estimated to be 0.1 μg l^{-1} simazine for a confidence range of 99.7% (3σ) assuming a mean σ of 4% of the blank value.

4. Summary and conclusions

We have investigated two different integrated optical devices based on an MZI structure with respect to their performance as immunoprobes. Highly improved performance

for the MZI device combined with a 3 × 3 coupler was found. One advantage was the possibility for referencing coupling instabilities with respect to the sum of all three outputs. Furthermore, optimum sensitivity and unambiguous detection of the direction of refractive index changes are achieved due to the phase shift between the three outputs. Suitable surface modification for label-free detection of antibody binding was applied and characterized with respect to non-specific and specific interaction. An antibody concentration of 7 nM was found to be adequate for carrying out an immunoassay calibration. A detection limit of 0.1 ppb simazine was found for the immunoassay using the improved device. This performance is excellent in comparison with other label-free techniques, but not yet suitable for the analysis of drinking water. However, this detection limit is sufficient for threshold detection in water quality control. The total assay time is already less than 20 min, but could readily be reduced to 5–10 min. As minimum sample pre-treatment is required, this method provides a rapid tool for monitoring applications.

The use of integrated optical techniques provides a potential for high parallelization. As established manufacturing techniques were used and dramatic simplification of the set-up is possible, we believe that we have presented an attractive perspective for further development of a label-free immunoprobe.

Acknowledgements

This research was supported by the EC environmental program, project BIOPTICAS (no. 5V-CT92-0067). Anti-triazine antibodies and Fab fragments and a triazine derivative were kindly supplied by Dr Ram Abuknesha, GEC Marconi Materials Technology, Hirst Division, Borehamwood, UK. The Optoelectronics Research Centre is funded by the UK EPSRC.

References

[1] C.P. Price and D.J. Newman (eds.), *Principles and Practice of Immunoassay*, Stockton Press, New York, 1991.

[2] F.F. Bier and R.D. Schmid, Real time analysis of competitive binding using grating coupler immunosensor for pesticide detection, *Biosensors Bioelectron., 9* (1994) 125–130.

[3] M. Minnuni and M. Mascini, Detection of pesticide in drinking water using real-time biospecific interaction analysis (BIA), *Anal. Lett., 26* (1993) 1441–1460.

[4] A. Brecht, J. Piehler, G. Lang and G. Gauglitz, A direct optical immunosensor for atrazine detection, *Anal. Chim. Acta, 311* (1995) 289–299.

[5] E.F. Schipper, R.P.H. Kooyman, R.G. Heideman and J. Greve, Feasibility of optical waveguide immunosensors for pesticide detection: physical aspects, *Sensors and Actuators B, 24* (1995) 90–93.

[6] M. Tom-Moy, R.L. Baer, D. Spira-Solomon and T.P. Doherty, Atrazin measurement using surface transverse wave devices, *Anal. Chem., 67* (1995) 1510–1514.

[7] C. Mouvet, L. Almaric, S. Broussard, G. Lang, G. Brecht and G. Gauglitz, Reflectometric interference spectroscopy for the determination of atrazine in natural water samples, *Environment. Sci. Technol.*, (1996) in press.

[8] B. Liedberg, C. Nylander and I. Lundström, Surface plasmon resonance for gas detection and biosensing, *Sensors and Actuators, 4* (1983) 299–304.

[9] W. Lukosz, Principles and sensitivities of integrated optical and surface plasmon sensors for direct affinity sensing and immunosensing, *Biosensors Bioelectron., 6* (1991) 215–225.

[10] R. Cush, J.M. Cronin, W.J. Stewart, C.H. Maule, J. Molloy and N.J. Goddard, The resonant mirror: a novel optical biosensor for direct sensing of biomolecular interactions. Part I: principle of operation and associated instrumentation, *Biosensors Bioelectron., 8* (1993) 347–353.

[11] R.G. Heideman, R.P.H. Kooyman and J. Greve, Performance of a highly sensitive optical waveguide Mach–Zehnder interferometer immunosensor, *Sensors and Actuators B, 10* (1993) 209–217.

[12] Ch. Stamm and W. Lukosz, Integrated optical difference interferometer as refractometer and chemical sensor, *Sensors and Actuators B, 11* (1993) 177–181.

[13] C. Mouvet, R.D. Harris, C. Mariac, B.J. Luff, J.S. Wilkinson, J. Piehler, A. Brecht, G. Gauglitz and R. Abuknesha, Determination of simazine in water samples by waveguide surface plasmon resonance, *Anal. Chim. Acta*, submitted for publication.

[14] J.A. De Feijter, J. Benjamins and F.A. Veer, Ellipsometry as a tool to study the adsorption behaviour of synthetic and biopolymers at the air–water interface, *Biopolymers, 17* (1978) 1759–1772.

[15] K. Spaeth, A. Brecht and G. Gauglitz, Studies on the biotin–avidin multilayer adsorption by spectroscopic ellipsometry, *J. Colloid Interface Sci.*, submitted for publication.

[16] W. Karthe and R. Müller, *Integrierte Optik*, Geest und Portig, Leipzig, 1991, p. 213.

[17] J. Ingenhoff, B. Drapp and G. Gauglitz, Biosensors using integrated optical devices, *Fresenius' Z. Anal. Chem., 346* (1993) 580–583.

[18] M. Heming, B. Danielzik, J. Otto, V. Paquet and C., Fattinger, Plasma impulse CVD deposited TiO_2 waveguiding films: properties and potential applications in integrated optical sensor systems, *Mater. Sci. Eng., A140* (1991) 733–740.

[19] B.J. Luff, R.D. Harris, J.S. Wilkinson, R. Wilson and D.J. Schiffrin, Integrated optical directional coupler biosensor, *Optics Lett., 21* (1996) 618–620.

[20] J. Piehler, A. Brecht, K.E. Geckeler and G. Gauglitz, Surface modification for direct immunoprobes, *Biosensors Bioelectron., 11* (1996) 579–590.

[21] G. Lang, A. Brecht and G. Gauglitz, Characterisation and optimisation of an immunoprobe for triazines, *Fresenius' Z. Anal. Chem., 354* (1996) 857–860.

[22] R.W. Glaser, Antigen–antibody binding and mass transport by convention and diffusion to a surface: a two-dimensional computer model of binding and dissociation kinetics, *Anal. Biochem., 213* (1993) 153–161.